ELSEVIER

Journal of Orthopaedic Research 22 (2004) 1336–1344

Journal of Orthopaedic Research

www.elsevier.com/locate/orthres

Production of consistent crush lesions in murine quadriceps muscle—A biomechanical, histomorphological and immunohistochemical study

Jonathan R. Bunn, John Canning, George Burke, Moses Mushipe, David R. Marsh, Gang Li *

Trauma Research Group, Department of Trauma and Orthopaedic Surgery, Queen's University Belfast, Musgrave Park Hospital, Stockman's Lane, Belfast BT9 7JB, Northern Ireland, UK

Received 1 March 2004; accepted 11 March 2004

Abstract

Poor healing of high-energy fractures is often associated with severe muscle damage. This may be partly due to the production, by the injured muscle, of inflammatory cytokines that somehow misdirect bone healing. In order to investigate this question, an animal model was established which embodies a controlled degree of muscle injury with a dose response to the energy absorbed, that can be characterised histologically. Using a custom crush jig, 60 CFLP mice had either 100 or 200 g masses dropped from a fixed height onto the quadriceps muscle, with mechanical measurement of the impact. Energy of impact was reliably and significantly different between the small and large impact conditions, though there was more variability when the large mass was used. Animals were sacrificed at day 2, 4, 8, 16, and 24 post-injury. Muscle histomorphometry at all time points and immunohistochemistry for IL-1β, IL-6, and TNF-α up to day 8 were used as measures of muscle damage, inflammation and repair. Histological sections were analysed into areas of normal muscle fibres, damaged/regenerating muscle fibres and fibrous/inflammatory infiltrate. Early histological response was similar between the two groups; the large crush group displayed significantly greater areas of inflammatory infiltrate and damaged muscle at the later time points after day 8. In the large crush group, IL-1β and IL-6 expression were significantly higher at day 2 and TNF-α was higher at day 8 when compared to the small crush group.

The experiment demonstrated that more severe injury to muscle was reliably followed by increased inflammatory cytokine production and a greater degree of inflammation and fibrosis. Increased production of inflammatory cytokines such as TNF-α and IL-1β in the damaged muscles may activate macrophages and recruit fibroblasts, promote scar formation and lead to delayed union or non-union of the adjacent fracture(s).

Keywords: Injury; Repair; Muscle; Cytokines; IL-1β; IL-6; TNF-α

Introduction

Poor healing in high-energy fractures is often associated with marked concomitant muscle injury. Classifications by Tscherne [15] and Gustilo [4] offer guidance to orthopaedic surgeons faced with such injuries, mainly based on the importance of the vascularity contributed by a healthy muscle bed both to underlying bone and overlying skin [10,17]. However the consequences of inflammation, the initiator of all healing, are often underemphasised when examining the role of injured muscle in healing.

In all types of muscle injury the cellular sequence of events is remarkably similar. Best et al. [1] have noted the similarities between muscle regeneration following injury and those during growth and development. Following injury, these satellite cells migrate to the site of disruption, proliferate, fuse with myotubes and become mature myofibrils [2,12]. The removal of dead and damaged muscle components is effected by endogenous proteases and by exogenous proteases released from infiltrating neutrophils and macrophages. An adequate blood flow is required for transport of inflammatory cells to the injury site. Twelve hours following injury,

* Corresponding author. Tel.: +44-2890-902830; fax: +44-2890-66111.

E-mail address: g.li@qub.ac.uk (G. Li).

0736-0266/$ - see front matter © 2004 Orthopaedic Research Society. Published by Elsevier Ltd. All rights reserved.
doi:10.1016/j.orthres.2004.03.013

macrophages represent the predominant inflammatory cell type [16]. Fibroblasts also mediate inflammation. They are stimulated by IL-1β and TNF-α from their normally quiescent state to produce collagen [8]. Allied to this they are capable of degrading extracellular matrix molecules and forming fragments known to be chemoattractive to both fibroblasts and inflammatory cells [1,13].

The balance, between inflammation of a degree necessary to initiate regeneration and excessive inflammation associated with poor muscle healing, scar formation and delayed fracture union, may be reflected in the production of inflammatory cytokines such as IL-1β and TNF-α [14]. A model embodying controlled variation in the degree of inflammatory response, with examination of morphology and underlying cytokine expression, would provide useful insights into the role of inflammation in repair. Our objective was to create a model which represents severe soft tissue envelope injury seen in high-energy trauma. We hypothesised that severe injury to muscle may cause excessive inflammatory cytokine production and that this might contribute to impaired muscle regeneration followed by scar formation and fracture healing.

Materials and methods

Development of muscle crush jig

A crush jig was developed (Fig. 1A and B) to drop a mass from a height of 130 mm onto the quadriceps muscle of an anaesthetised mouse. This consisted of a mass suspended beneath an electromagnet, and a guide rod down which the mass dropped to impact onto a flange at the lower end of the rod. The lower tip of the guide rod rested on the upper limb of a pair of crush forceps (Fig. 1C), the jaws of which contained the muscle to be crushed.

Measurement of the impact was carried out on the empty jaws of the crush forceps. A 20 kg load cell supporting the crush forceps on an aluminium trestle transduced the impact into an electrical signal, which was amplified and captured on a PC using an analogue/digital converter and high frequency sampling software. In a pilot study impact measurement was then performed on the quadriceps of ten mice: five with a 100 g weight and five with a 200 g weight. The energy of the measured impacts was derived and energy per unit volume of crushed tissue was calculated and recorded.

Surgical procedure

All animal experimental procedures were approved and performed under the control of guidelines for the Animals (Scientific Procedures) Act 1986, British Home Office.

For the main study 60 skeletally mature (35–45 g) male CFPL mice were used. Half had a small crush (100 g mass) and half had a large crush (200 g mass). Mice under general anaesthesia and aseptic conditions had a lateral incision through shaved skin and fascia lata from the left knee to the greater trochanter. The plane between the vastii and

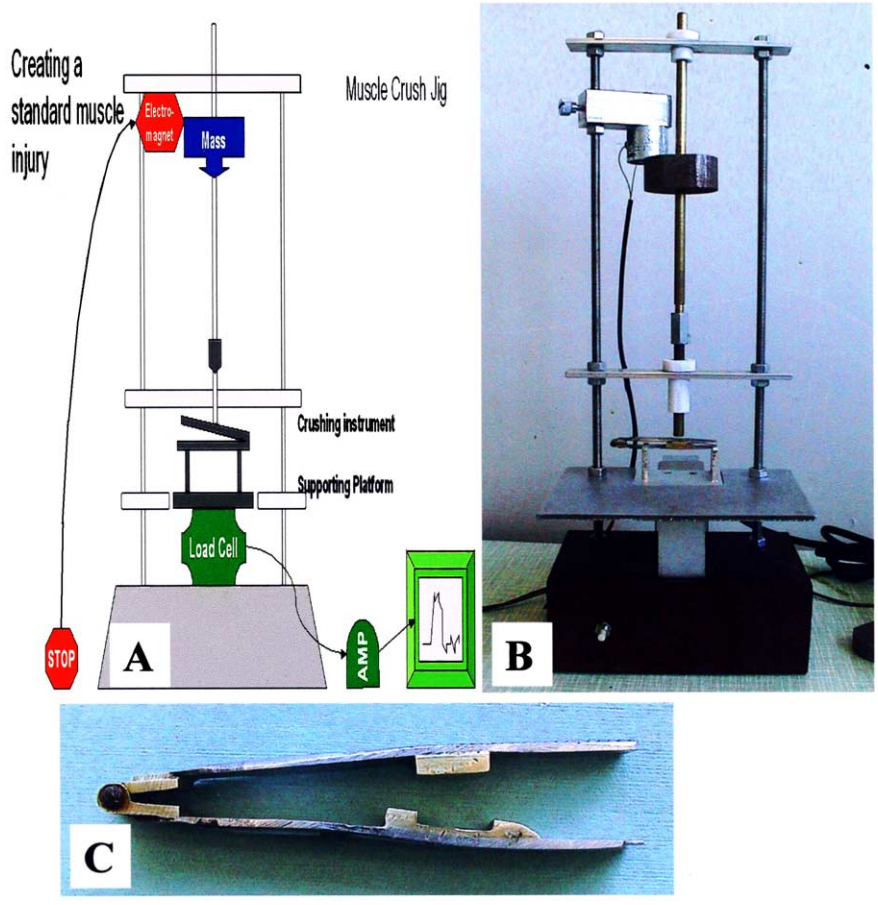

Fig. 1. Crush jig with crush forceps in situ (A) schematic (B) the crush jig, and (C) the crush forceps.

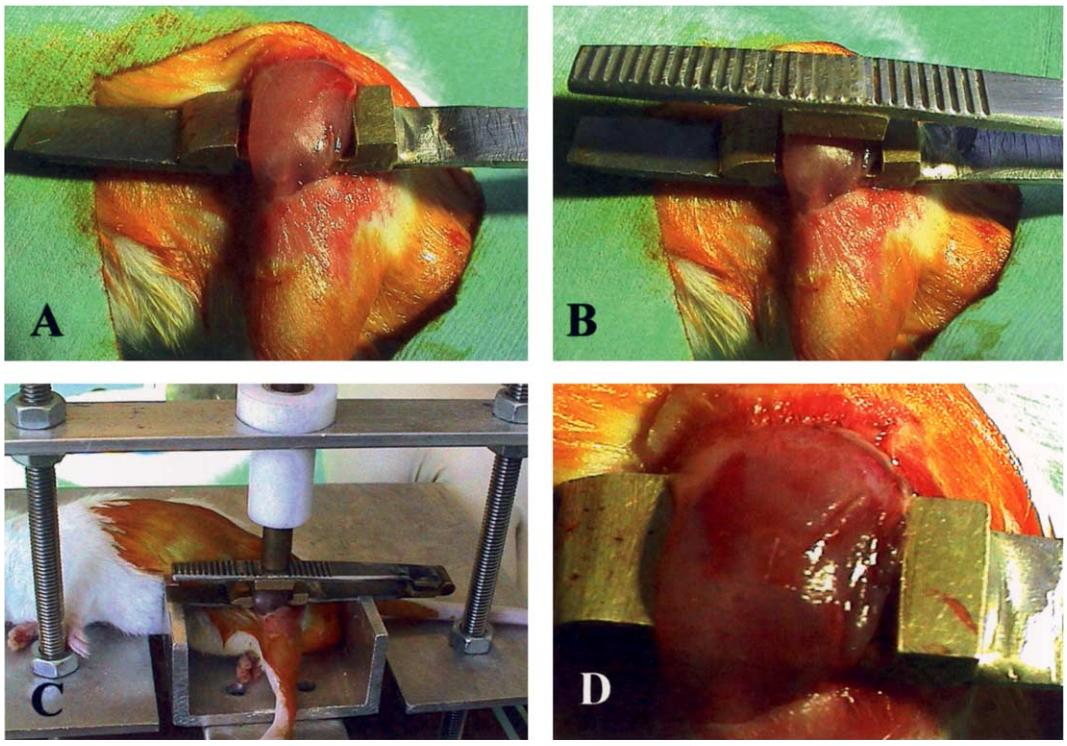

Fig. 2. (A) Crush forceps with profile designed to constrain muscle fibres within the jaws. (B) Crush forceps in situ prior to positioning in the crush jig. (C) Positioning of mouse with crush forceps in situ in the crush jig. (D) Appearance of the muscle belly immediately after crush injury.

hamstrings was opened by blunt dissection to expose the femur. A tissue plane was opened in a coronal plane beneath the quadriceps so that the body of the muscle was separated from underlying femur. The lower jaw of the crush forceps was inserted between the quadriceps muscle and the femur, the top jaw resting gently on the superior surface of the muscle (Fig. 2A and B). An estimate of quadriceps cross sectional area was made by measuring the muscle width within the forceps and the muscle thickness between the upper and lower jaws of the forceps. The mouse with forceps in situ was placed on the crush jig and the weight allowed to fall and crush the quadriceps muscle as described above (Fig. 2C). The crushed muscle was gently lifted from the crush forceps (Fig. 2D) and the wound was closed. The animal was recovered and free cage activity was permitted for the experiment duration.

Sample preparation

Mice were sacrificed in groups of 6 at day 2, 4, 8, 16 and 24-post-muscle-crush. The left femur was excised by sharp dissection and disarticulation through the knee and hip joints with the overlying quadriceps muscle in situ. The quadriceps muscle was then retrieved, releasing through the quadriceps tendon distally and across uninjured muscle proximally. Following excision the muscle specimens were coded and fixed in 10% buffered formalin for 48 h. They were processed for paraffin histology and subsequently embedded in paraffin wax. Six micrometers thick sections were cut in the central coronal plane of the samples and were mounted on poly-L-lysine (Sigma Chemical Co., UK) coated slides. They were then stained with haematoxylin and eosin. Sections for immunocytochemistry staining were similarly cut and a standard indirect peroxidase method was used for staining for IL-1β, IL-6 and TNF-α. Briefly, we cleared the paraffin with xylene twice for 10 min and then rinsed the slides twice for 2 min each in graded alcohols (100%, 95%, 70%, 50% ethanol) through to PBS (pH 7.2) for 5 min. Antigen retrieval was performed using proteinase-K solution (20 μg/ml, DAKO, Dorset, UK) for 30 min at 37 °C followed by blocking of endogenous peroxidase using 3% H_2O_2 solution for 10 min. Sections were washed three times for 2 min with PBS and the primary antibody (Table 1) was applied for 1 h at 1:50 dilution at room temperature in a humidified chamber. Slides were rinsed three times in PBS and secondary antibodies (Table 1) at 1:100 dilution were applied for 1 h at room temperature in a humidified chamber. The HRP conjugated secondary antibodies were visualised using DAB substrate/chromagen solution for 1–5 min.

Table 1
Primary and secondary antibodies used for detection of IL-1β, IL-6, and TNF-α

Primary antibody	Manufacturer	Source/type	Species	Dilution
IL-1β	Serotec	Rabbit monoclonal IgG	Rabbit monoclonal IgG	1:50
IL-6	Serotec	Rabbit monoclonal IgG	Rabbit monoclonal IgG	1:50
TNT-α	Serotec	Rabbit monoclonal IgG	Rabbit monoclonal IgG	1:50
			Disclosure	
IL-1β	Dako	Goat anti-Rabbit	HRP—DAB	1:100
IL-6	Dako	Rabbit anti-Rat	Biotin—DAB	1:100
TNF-α	Dako	Rabbit anti-Rat	Biotin—DAB	1:100

Image analysis

All coded sections were analysed blindly. Each section was viewed by light microscopy (Leica DMLB; Leica Microscopy Systems, Heerburg, Switzerland). Three digital images were taken of the central damaged muscle zone in each specimen using Kodak Digital Sciences DC120 200M camera and Digital Access (TWAIN Acquire) software (Eastman Kodak Company, 1997). The images were then imported into image analysis software Bioquant Nova Version 4.00.8 Advanced Image Analysis (© 2001 R&M Biometrics, Inc, TN, USA), and the area staining positively for cytokine was measured in pixels.

From the H&E stained slides, it was possible to distinguish between normal and abnormal muscle fibres, but not possible to distinguish between dying fibres and those regenerating. Similarly, among infiltrating small round cells, it was not possible to distinguish between fibroblasts and inflammatory cells. Areas of normal undamaged muscle, damaged/regenerating muscle and fibrous/inflammatory infiltrate were defined and quantified as numbers of pixels, averaged between three images per specimen.

Statistical analysis

The histomorphometric results were compared between large and small crush groups at all time-points. Data were entered into an SPSS (v.11) data file and non-parametric methods were used, displaying distributions by means of boxplots and comparing groups with the Mann-Whitney U test.

Results

Mechanical measurements

Energy of impact of 100 and 200 g weights onto empty crush forceps demonstrated a highly significant difference between groups ($p < 0.001$, Student's t-test), with a high degree of consistency within each group. Comparison of the relative energy absorbed by unit volume of muscle during the small and large crush was also found to be highly significantly different ($p = 0.009$, Student's t-test). There was more variability in the high-impact group, possibly due to the increased likelihood of a bounce following impact and alterations in the viscoelastic properties of the muscle as it was deformed more severely.

Muscle appearance

There were no significant differences in mean weights and mean quadriceps muscle cross sectional area between groups showed. Comparison of macroscopically the difference between the small and large crush group was evident from the time of impact onwards. Whilst we made no attempt to quantify the differences, we observed increased haemorrhage, oedema and muscle disruption in the large crush group compared with the small crush group. When harvesting the muscle we found the haematoma formation, oedema and persistence of bruising extended beyond eight days in the large crush group while in the small crush group there was little evidence of haematoma or oedema by eight days. By 16 days the large crushed muscle group showed persistent oedema with a pale scarring central zone appearing in the muscle belly, the small crush group looked virtually normal. At 24 days the large crush group had a clearly demarcated central zone of fibrous scarring compared with the normal appearance of the small crush muscle at this time.

Histomorphometry analysis

Morphological alterations in the muscle architecture were seen from day 2 onwards (Fig. 3). Loss of striations, swelling of myofibres, vacuolisation and internalisation of nuclei were seen in small and large crush injuries at day 2 (Fig. 3A and B). A brisk inflammatory infiltrate and fibroblast proliferation followed at day 4 (Fig. 3C and D), before myofibre regeneration and resolution occurred at day 24 (Fig. 3E and F). Three parameters were used to measure the effect of crush on the muscle; the area of damaged or regenerating fibres, the area of infiltrating inflammatory or fibrous tissue and the area of intact fibres.

The areas of damaged and regenerating muscle were consistently higher in the large crush group compared with the small crush group across the duration of the experiment (Fig. 4A), reaching significance at later time-points at day 16 and day 24 ($p < 0.05$, Mann-Whitney U test). We noted a substantial increase in damaged fibres in the large crush group between day 2 and day 4, possibly representing a local ischaemic-reperfusion effect as activated inflammatory cells became able to penetrate the central zone of the crush and produce more toxic molecules which damaged potentially viable cells. This change was not seen in the small crush group, and by day 16 it could be clearly seen that regeneration was almost complete in the small crush group with few regenerating fibres or inflammatory/fibrous cells within the muscle. In contrast 30% of the fibres in the large crush group still had the morphological features of regenerating muscle fibres. This observation persisted at day 24 reaching significance at the $p = 0.05$ level (Fig. 4A).

The inflammatory infiltrates and fibroblast invasion peaked rapidly at day 8 in the small crush group (Fig. 4B) as inflammatory mediators recruit and activate neutrophils and macrophages from the circulation. As soon as the necrotic cellular debris was removed the inflammatory cells disappeared, corresponding with the maximal regeneration of the muscle fibres. After day 8 in the small muscle crush group, there were few inflammatory/fibrous cells within the muscle fibres and virtual normal morphology was seen. The large crush group showed steady rise in invading inflammatory cells, peaking at day 16 and remaining well sustained above small crush levels beyond this time point (Fig. 4B). The slow peak of the inflammatory infiltrates was in contrast to the rapid peak seen in the small crush and was

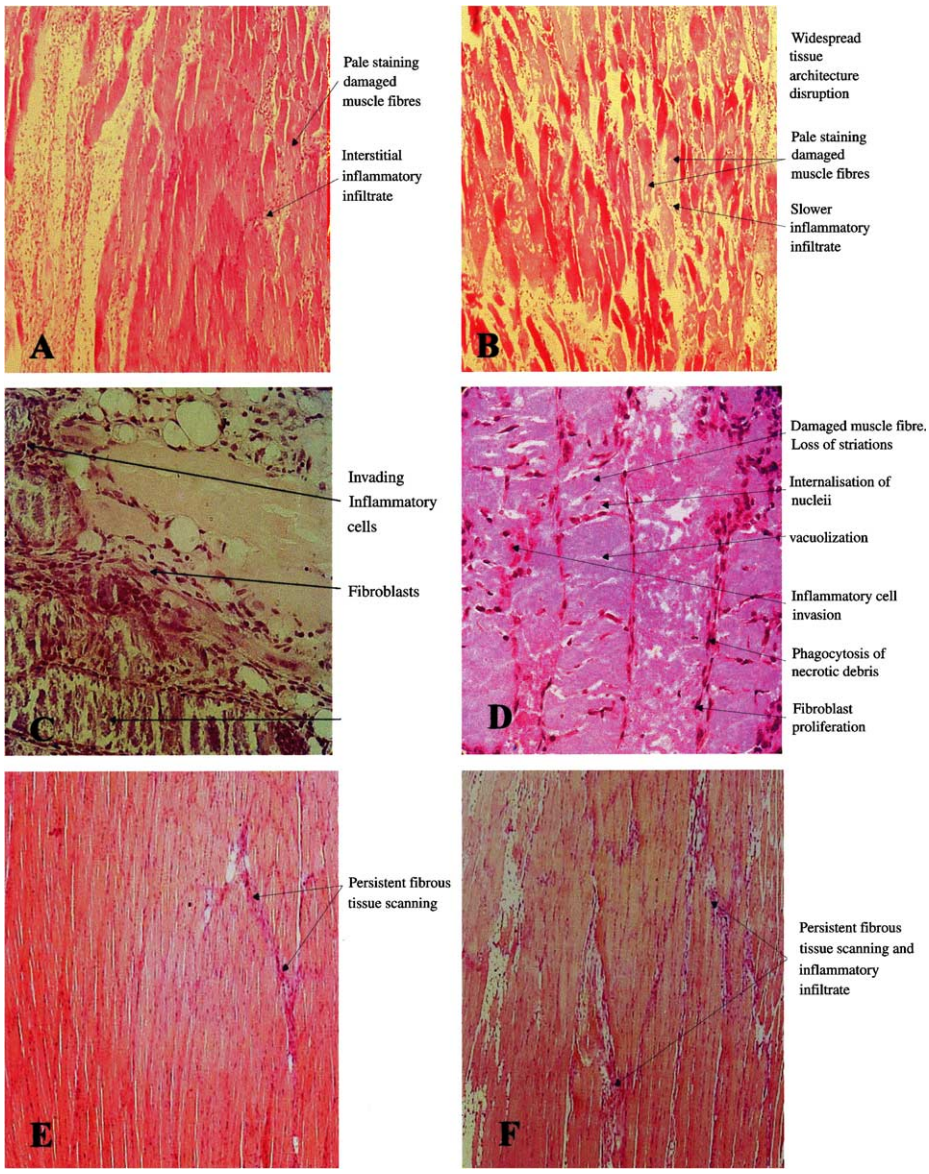

Fig. 3. (A) Histology of muscles crushed by 100 g masses and (B) by 200 g masses at day 2 post-injury, note the substantial disruption of fibre architecture and absence of inflammatory infiltrate in the muscles with large crush masses (arrows). (C) In the small muscle crush samples at day 4, necrotic muscle fibres were seen adjacent to damaged fibre, with many invading inflammatory cells and fibroblasts (arrows). (D) In the large muscle crush samples at day 4, muscle fibre degeneration, loss of striations, internalisation of nuclei, inflammatory cell invasion were clearly evident (arrows). (E) In the small crushed muscles at day 24, there were some fibrous scarring tissues present, but the inflammatory infiltrates were scarce. (F) In the large crushed muscles at day 24, a large amount of fibrous scarring tissues were present with numerous inflammatory infiltrates. H&E staining, A, B, E, F, ×100 magnifications; C and D, ×400 magnifications.

surmised to be attributable to damage to vascular conduits leading to the centre of the large crush area.

The area of intact uninjured muscle showed the differential effect of a large versus small muscle crush. At early time-points the area of intact muscle was greater in small muscle crush samples, similarly after day 8, showing significant differences at day 16 and day 24 ($p < 0.05$, Mann-Whitney U test). At the end of the experiment the small crush had regenerated over 95% to normal muscle while the large crush group could only manage 60%.

Immunohistochemistry

Immunohistochemistry for IL-1β, IL-6, and TNF-α were semi-quantified by expressing the area of positive staining material in three ×200 fields in pixels and comparing between groups. Standard deviations within groups were large owing to the variability of this technique, however interesting trends were seen.

IL-1β was expressed in all samples. Expression appears predominantly within and around invading inflammatory cells in the extracellular space. The

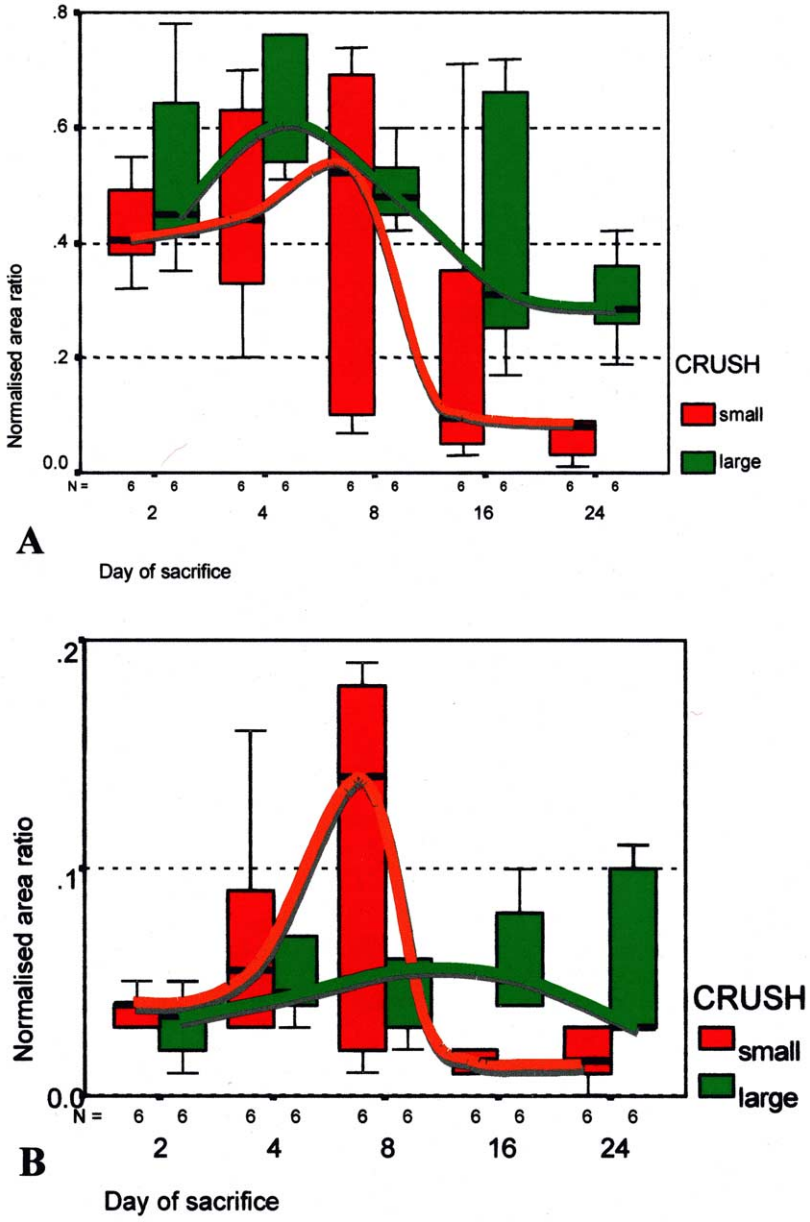

Fig. 4. (A) Diagram representing areas of damaged and regenerating muscle fibres within the large and small muscle crush groups. Regeneration was maximal in the small crush group at day 8, but it rapidly returned to normal morphology at day 16. In the large crush muscles, regeneration persisted through the experimental period, and at day 24 regenerating muscle fibres only constituted 30% of the muscle fibre bulk. (B) Diagram representing areas of inflammatory and fibrous infiltrate within crushed muscles. In the muscles received small crush, a rapid peak of inflammatory infiltrates was seen at day 8, and returned to basal levels at day 16. In the muscles received large crush, they contained fewer infiltrating inflammatory cells at day 2 and 4 post-injury, but the inflammatory cells remained in the tissue for longer duration.

inflammatory cells were predominantly monocyte/macrophage morphologically (Fig. 5A). A rapid peak in expression was seen in small muscle crush samples at the day 4 post-injury followed by a rapid fall (Fig. 5B); however, the expression pattern in the large crush group showing an moderately increased expression at day 4 and a further moderate increase in expression at day 8 (Fig. 5B). In the large crush group the expression may peak even later than day 8 suggesting that inflammation responses was delayed but more sustained in this group (Fig. 5B).

TNF-α was expressed in all samples (Fig. 5C). In the small muscle crush groups the expression mirrored the expression of IL-1β, peaking at day 4 and rapidly returning towards normal at day 8 (Fig. 5D). In contrast the large crush group exhibited increased expression of TNF-α at each time-point, consistent with the expression of IL-1β. Again the large crush group seemed to

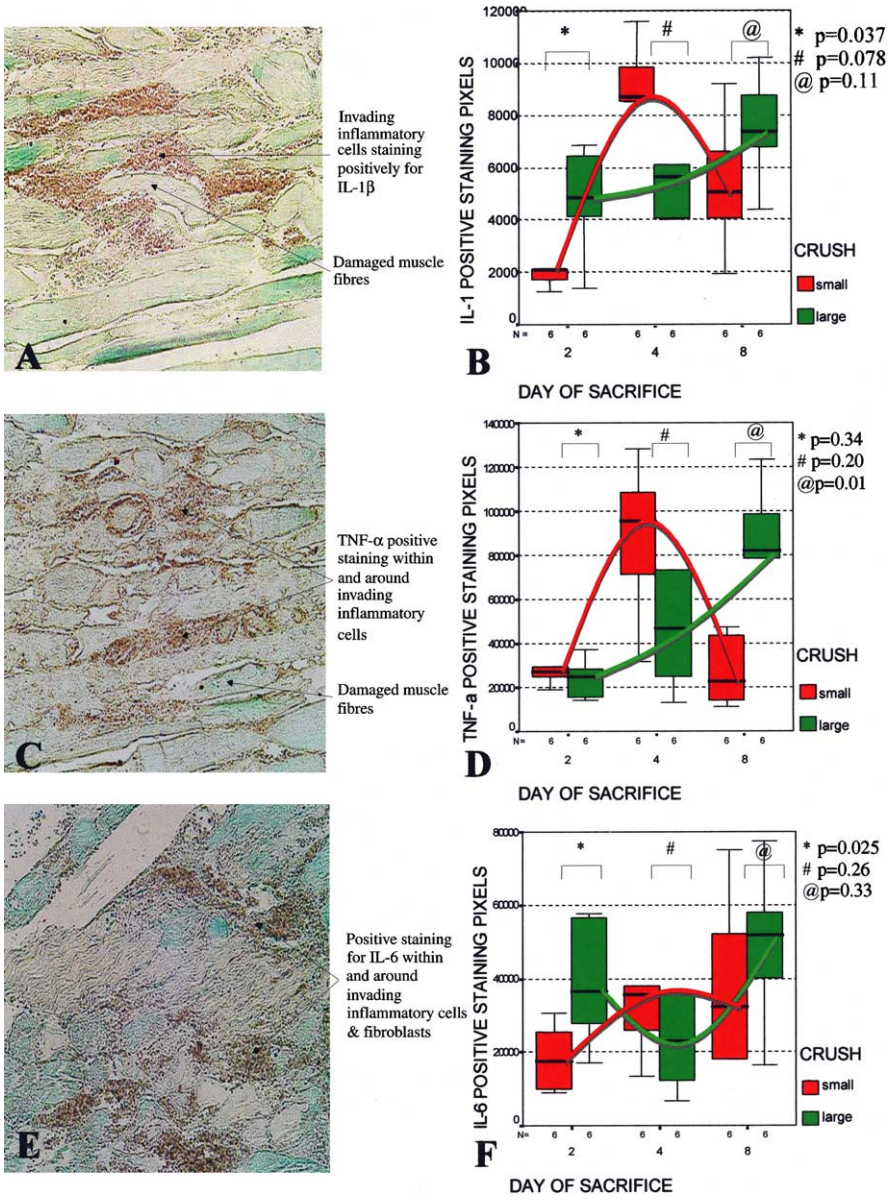

Fig. 5. (A) Example of IL-1β ICC in the muscles with large crush at day 4, IL-1β expression appeared predominantly in or around invading inflammatory cells in the extracellular space. (B) Diagram showing semi-quantitative expression of IL-1β in the small and large crush groups with time. (C) Example of TNF-α ICC in the muscles with large crush at day 4, TNF-α expression was similar as the IL-1β expression, TNF-α positive staining were mostly seen in the fibrous and inflammatory interstitial infiltrates. (D) Diagram showing semi-quantitative expression of TNF-α in the small and large crush groups with time. (E) Example of IL-6 ICC in the muscles with large crush at day 4, showing that fibrous tissue and invading inflammatory cells were both potent sources of this cytokine. (F) Diagram showing semi-quantitative expression of IL-6 in the small and large crush groups with time. Statistical analysis in B, D, and F was performed using Mann-Whitney U test for unpaired data, with p values stated respectively.

have a delayed but much more sustained inflammatory reaction within the injured muscle (Fig. 5D).

IL-6 was expressed in all samples (Fig. 5E). The small crush group demonstrated no significant change in expression at sequential time-points but had a tendency to peak at day 4 and then returned towards to baseline levels (Fig. 5F). IL-6 expression increased in the large crush groups at day 8, this was linked with the presence of inflammatory and fibrous tissue and may persist at high levels for some time after this (Fig. 5F).

Discussion

This study was the first stage in the development of a clinically relevant model of high-energy trauma, which will incorporate a reliable degree of damage to the soft tissue envelope around an underlying fracture. Its purpose was to develop a mechanism that reproducibly insults the quadriceps muscle of a mouse with a crush injury and predictably causes a differential healing response between small and large crushes. The variables in

which reliability was sought were (i) the energy transmitted through the muscle, (ii) proportions of inflammatory/fibroblast infiltration and damaged/regenerating muscle and (iii) expression of the inflammatory cytokines TNF-α, IL-1β and IL-6. This model is potentially useful to study the effects of high-energy trauma on muscle and fracture repair; and mechanisms of fracture non-union and its treatment by blocking the inflammatory cytokines using neutralizing antibodies.

Measurement of the impact onto muscle demonstrated reasonably consistent impacts within each group. The mean energy of impact per unit volume of tissue was exactly double in the large crush group. The greater variability energy of impact in the large crush may be explained by the bounce of the larger mass following the drop. Histomorphometry remains the gold standard for measurement of muscle damage [11]. The areas of uninjured muscle, damaged-regenerating muscle and inflammatory and fibrous infiltrate clearly show the differential effect of a large versus small muscle crush. Within groups a predictable and reproducible pattern of healing emerged. These parameters clearly differentiated the effects of a small crush from a large crush at later time-points. We therefore consider this model to provide a reliable means of injuring muscle.

Following injury there was a substantial decrease in the area of intact muscle at day 4 in the large crush group corresponding with a substantial rise in the area of damaged fibres. This confirms that a damaging stimulus is ongoing in the muscle four days after the impact. This is possibly due to a local reperfusion type injury or 'second hit phenomenon' in which the severe injury activates inflammatory cells and as a consequence more damage is caused when the inflammatory cells invade areas of normal and necrotic tissue [5,14]. This was not seen in the small crush samples. The fibrous and inflammatory infiltrate in the small crush group was peaked rapidly and equally briskly diminished, exceeding the infiltrate seen in the large group. No collateral damage was observed in the small crush group. In contrast the large crush group had a slow delayed peak infiltrate that persisted and resulted in ongoing regenerating muscle fibres until day 24. Jarvinen and Sorvari [7] observed three distinct zones in their crush model which are replicated in our severe crush group: a central zone with few invading cells, a penumbra of regenerating fibres full of inflammatory and fibrous cells and a surrounding intact envelope. It is apparent from our histologic observations that the slow peak is in contrast to the rapid peak seen in the small crush and is surmised to be attributable to damage to vascular conduits leading to the centre of the large crush area.

Muscle regeneration depends on angiogenesis. At two days post-injury, sprouting capillaries are seen growing in from the periphery of the damaged site, producing granulation tissue by five days. Should the centre of the injured area lie too far from an intact blood supply, it is not revascularised and becomes replaced with scar tissue, without myotube regeneration [3]. Excessive connective tissue production inevitably leads to scarring and fibrosis. Inflammatory cytokines TNF-α and IL-1β are chemoattractive for neutrophils, macrophages and fibroblasts. These cells are necessary in the early inflammatory response to scavenge and remove necrotic material, preparing for mesenchymal proliferation and revascularization [6]. The expression of inflammatory cytokines IL-1β and TNF-α in the small crush group peaked at day 4 and rapidly returned towards normal levels. This triggered the rapid increase in inflammatory infiltrate seen between day 4 and day 8 in the small crush group and subsequent rapid disappearance. This is in contrast with the expression in the large crush group, which continues to demonstrate a rising expression at day 8 and correspondingly an ongoing inflammatory presence. We see no clear differences in IL-6 expression but the differential expression of IL-1β and TNF-α (significant at day 8) must dictate the morphological differences after this point. It is possible that a persisting inflammatory stimulus is present (cellular debris etc.) or that a continuing local environment rich in inflammatory cytokines, inflammatory cells and activated fibroblasts and poorly perfused with nutrients and oxygen exists. This prevents the regeneration of myotubules and promotes the formation of scar tissue.

These observations permit some understanding of mechanisms underlying such a divergent healing response seen not only in fractures with adjacent soft tissue envelope trauma, also in spine surgeries with prolonged instrumentation that caused muscle damages and subsequent server pain and stiff back. Clearly this is an oversimplification and other cytokines and growth factors may also be involved, such as TGFβ, FGF, IGF [9]. It may also be hypothesized that a defect in angiogenic response or vascular mechanism may be responsible for scar formation in injured muscles. Further investigations are warranted to test these hypotheses in different clinical settings.

In conclusion, the muscle crush model described above was reproducible as demonstrated by the highly repeatable measured impacts. Reliability was seen in statistically clear histomorphometric differences between the two groups and corresponding ICC findings which substantiated the morphological changes observed. Validity was supported by corroborating findings from other authors of muscle crush injury models and in clinical experience of the effects of high-energy soft tissue injuries and their complications compared with low energy injuries. IL-1β and TNF-α were persistently elevated in the large crush samples and they may be associated with increased scar formation and poor fracture healing. This model may be useful for further studies on

the mechanisms/treatments of impaired fracture healing associated with soft tissue envelope injuries.

Acknowledgements

This work was funded by research grants from the R&D Office, Department of Health and Social Services, Northern Ireland (EAT/1171/99) to JRB, GL and DRM.

References

[1] Best TM, Hunter KD. Muscle injury and repair. Phys Med Rehabil Clin N Am 2000;11(2):251–66.
[2] Fisher BD, Baracos VE, Shnitka TK, Mendryk SW, Reid DC. Ultrastructural events following acute muscle trauma. Med Sci Sports Exerc 1990;22(2):185–93.
[3] Grounds MD. Towards understanding skeletal muscle regeneration. Pathol Res Pract 1991;187(1):1–22.
[4] Gustilo RB, Anderson JT. Prevention of infection in the treatment of one thousand and twenty-five open fractures of long bones: retrospective and prospective analyses. J Bone Joint Surg Am 1976;58(4):453–8.
[5] Gute DC, Ishida T, Yarimizu K, Korthuis RJ. Inflammatory responses to ischemia and reperfusion in skeletal muscle. Mol Cell Biochem 1998;179(1–2):169–87.
[6] Husmann I, Soulet L, Gautron J, Martelly I, Barritault D. Growth factors in skeletal muscle regeneration. Cytokine Growth Factor Rev 1996;7(3):249–58.
[7] Jarvinen M, Sorvari T. Healing of a crush injury in rat striated muscle. 1. Description and testing of a new method of inducing a standard injury to the calf muscles. Acta Pathol Microbiol Scand [A] 1975;83(2):259–65.
[8] Kovacs EJ, DiPietro LA. Fibrogenic cytokines and connective tissue production. FASEB J 1994;8(11):854–61.
[9] MacGregor J, Parkhouse WS. The potential role of insulin-like growth factors in skeletal muscle regeneration. Can J Appl Physiol 1996;21(4):236–50.
[10] Rushton JL, Davies I, Horan MA, Mahon M, Williams R. Production of consistent crush lesions of murine skeletal muscle in vivo using an electromechanical device. J Anat 1997;190(Pt 3):417–22.
[11] Salmon S. Muscle damage. Oxford University Press; 1997.
[12] Schmalbruch H. The morphology of regeneration of skeletal muscles in the rat. Tissue Cell 1976;8(4):673–92.
[13] Sorichter S, Puschendorf B, Mair J. Skeletal muscle injury induced by eccentric muscle action: muscle proteins as markers of muscle fiber injury. Exerc Immunol Rev 1999;5:5–21.
[14] Tidball JG. Inflammatory cell response to acute muscle injury. Med Sci Sports Exerc 1995;27(7):1022–32.
[15] Tscherne H, Oestern HJ. A new classification of soft-tissue damage in open and closed fractures. Unfallheilkunde 1982; 85(3):111–5.
[16] Walker BE. Radioautographic investigations of muscular dystrophy in the mouse. Tex Rep Biol Med 1964;22(Suppl 1):940–3.
[17] Walton M, Rothwell AG. Reactions of thigh tissues of sheep to blunt trauma. Clin Orthop Rel Res 1983;(176):273–81.